SECOND EUROPEAN CONFERENCE ON EARTHQUAKE ENGINEERING AND SEISMOLOGY, ISTANBUL AUG. 25-29, 2014

TUNING OF STOCHASTIC GROUND MOTION MODELS FOR COMPATABILITY WITH GROUND MOTION PREDICTION EQUATIONS

Christopher VETTER[1], Alexandros TAFLANIDIS[2], George MAVROEIDIS[3] and Ioannis GIDARIS[4]

ABSTRACT

Stochastic ground motion models facilitate a versatile description of earthquake acceleration time-histories by modulating a stochastic (white-noise) sequence through functions that address spectral and temporal properties of the excitation. This is established by relating the parameters of these functions to earthquake and site characteristics through appropriate predictive relationships. This work focuses on the selection of these predictive relationships to establish a direct compatibility of the risk described through the resultant ground motions with the risk described by Ground Motion Prediction Equations (GMPEs). A record-based ground motion model is selected as a stochastic ground motion model and specific Next Generation Attenuation (NGA) models are targeted as GMPEs for this study. The goal is to offer a versatile, computational efficient approach that will provide ground motions that match specific GMPEs based on a set of seismicity characteristics (moment magnitude, rupture distance) and structural periods chosen to target for this match. Foundation of the methodology is the development of a metamodel to approximate the median predictions of the ground motion model. This is established by selecting a wide range for the parameters of the model, generating ground motions for each of them (for different white noise sequences) and then calculating the spectral acceleration for different structural periods. The variability due to the stochastic sequence is addressed by averaging (median response) over the ensemble of such sequences considered. Based on this database, a kriging metamodel is developed to provide an efficient approximation of the ground motion model predictions. This metamodel is then used to efficiently select the predictive relationships that optimize the match to any desired GMPE. This match is defined by comparing the error between the stochastic ground motion predictions and the GMPEs for any desired cases, with each case corresponding to a chosen moment magnitude, rupture distance and structural natural period.

INTRODUCTION

One of the most important aspects of seismic risk assessment is the characterization of the earthquake hazard through appropriate models that adequately address its variability for different seismicity levels while providing a seismic-excitation description appropriate for the application of interest. For applications involving dynamic analysis, this description corresponds to the entire ground motion

[1] Ph.D. Candidate, University of Notre Dame, Notre Dame, IN, U.S.A., cvetter@nd.edu
[2] Associate Professor, University of Notre Dame, Notre Dame, IN, U.S.A., a.taflanidis@nd.edu
[3] Assistant Professor, University of Notre Dame, Notre Dame, IN, USA, g.mavroeidis@nd.edu
[4] Ph.D. Candidate, University of Notre Dame, Notre Dame, IN, U.S.A., igidaris@nd.edu

acceleration time history. The growing interest in the last decade in performance-based earthquake engineering (PBEE) (Goulet, Haselton et al. 2007) and in simulation-based risk mitigation approaches (Au and Beck 2003; Taflanidis 2011) has increased the relevance of this need. PBEE addresses the entire spectrum of structural response, ranging from linear to nonlinear to structural collapse, requiring a realistic characterization of earthquake acceleration time histories. In parallel, simulation-based approaches provide a versatile framework for risk mitigation, especially for the design of high-performance protection systems such as floor and base-isolation systems and viscous dampers (Taflanidis and Jia 2011). Within this approach, a description of earthquake hazard in the form of acceleration time histories is needed for a realistic, comprehensive characterization of seismic risk.

Undoubtedly the most popular approach for accomplishing this task is the selection/scaling of ground motions based on Intensity Measures (IMs) (representing the dominant excitation features) for different hazard levels (Baker and Cornell 2005). Though popular, this approach suffers from the facts that (a) the inherent variability of the acceleration time history is somewhat arbitrarily addressed by the exact selection of the ground motions (Jalayer and Beck 2008), and that (b) a limited number of hazard levels can only be considered, which might not adequately capture the seismic risk for intermediate levels. More importantly, scientific concerns have been recently raised regarding the validity of ground motion scaling, as it was shown that this approach contributes to a significant bias in assessing seismic risk (Grigoriu 2011). This realization has motivated researchers in the structural engineering field to revisit and, perhaps, put greater emphasis on stochastic ground motion modeling for characterizing seismic hazard (Rezaeian and Der Kiureghian 2010; Dabaghi, Rezaeian et al. 2011; Gavin and Dickinson 2011; Yamamoto and Baker 2013; Vetter and Taflanidis 2014). These models are based on modulation of a stochastic sequence through functions that address spectral and temporal characteristics of the ground motion. The parameters of these functions (such as duration of excitation or parameters related to frequency content) can be related to seismicity and site characteristics by appropriate predictive relationships. Various frameworks have been proposed for developing such ground motion models, namely distinguishing between the approaches adopted for establishing the predictive relationships they involve. *Source-based* models (Boore 2003) rely on physical modeling of the rupture and wave propagation mechanisms whereas *record-based* models (Papadimitriou 1990; Rezaeian and Der Kiureghian 2008) are developed by fitting a preselected "waveform" to a suite of recorded ground motions. One critical concern related to these approaches is the fact that compatibility of the resultant ground motions with the seismic hazard for specific structures and sites is not necessarily obtained (Taflanidis, Vetter et al. 2013).

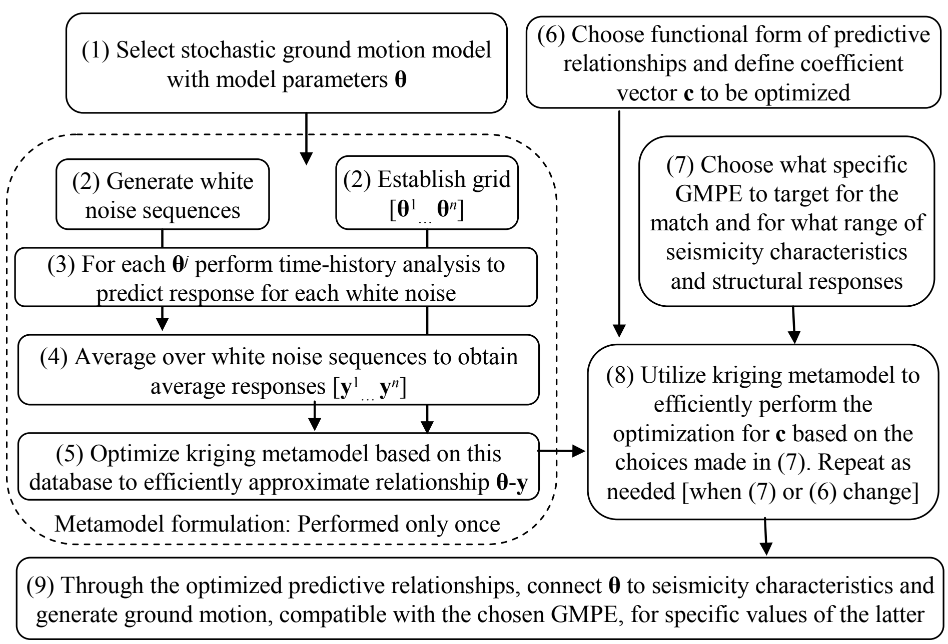

Figure 1. Schematic of the proposed implementation. Numbers in parenthesis indicate sequence of tasks.

Motivated by this realization this work focuses on the selection of the predictive relationships within stochastic ground motion modelling so that compatibility of the resultant ground motions with the spectral acceleration of Ground Motion Prediction Equations (GMPEs) is established, an idea initially presented by (Scherbaum, Cotton et al. (2006). Rather than targeting a priori a specific GMPE and seismicity characteristics for this compatibility, as in (Scherbaum, Cotton et al. 2006), a versatile framework is established in this study. Namely, a kriging metamodel is initially developed to approximate the stochastic ground motion model, based on an extensive database of predictions for the spectral acceleration for different model parameter properties. The development of this database involves a significant computational burden, but needs to be performed only once. The metamodel is then used to support an efficient optimization to select the values for the predictive relationships that optimize the match to GMPEs. This match is defined by comparing the error between the average (where this averaging relates to the influence of the white noise) stochastic ground motion predictions and the GMPEs for specific scenarios, with each scenario corresponding to a chosen moment magnitude, rupture distance or structural period. As soon as these scenarios are defined, the corresponding optimization can be performed very quickly, exploiting the computational efficiency of the kriging approximation as well as the opportunity to calculate gradients analytically, providing the opportunity to generate ground motions that match different characteristics. Figure 1 illustrates the general implementation scheme that will be presented next in this paper, starting with the details on the ground motion model chosen.

STOCHASTIC GROUND MOTION MODEL

The particular stochastic ground motion model chosen for this study is a record-based model which addresses efficiently both temporal and spectral non-stationarities. The discretized time history of the ground motion, $\ddot{a}_g(t)$, is expressed according to this model as (Papadimitriou, 1990; Rezaeian and Der Kiureghian, 2010)

$$\ddot{a}_g(t) = q(t,\boldsymbol{\theta})\left\{\sum_{i=1}^{k}\frac{h[t-t_i,\boldsymbol{\theta}(t_i))]}{\sqrt{\sum_{j=1}^{k}h[t-t_j,\boldsymbol{\theta}(t_j))]^2}}w(i\Delta t)\right\} \quad k\Delta t < t < (k+1)\Delta t \tag{1}$$

where $\mathbf{W} = [w(i\Delta t): i = 1,2,...,N_T]$ is a white noise sequence, Δt is the chosen discretization interval (assumed here constant and equal to 0.005 s), $q(t,\boldsymbol{\theta})$ is the time-modulating function, and $h[t-\tau,\boldsymbol{\theta}(\tau)]$ is an impulse response function corresponding to the pseudo-acceleration response of a single-degree-of-freedom (SDOF) linear oscillator with time varying frequency $\omega_f(\tau)$ and damping ratio $\zeta_f(\tau)$, in which τ denotes the time of the pulse

$$\begin{aligned} h[t-\tau,\boldsymbol{\theta}(\tau))] &= \frac{\omega_f(\tau)}{\sqrt{1-\zeta_f^2(\tau)}}\exp\left[-\omega_f(\tau)\zeta_f(\tau)(t-\tau)\right]\sin\left[\omega_f(\tau)\sqrt{1-\zeta_f^2(\tau)}(t-\tau)\right]; \quad \tau \le t \\ &= 0; \quad \text{otherwise} \end{aligned} \tag{2}$$

For the time varying characteristics, the following functions are adopted for the frequency and damping, as in (Beck and Papadimitriou 1993), leading to

$$\begin{aligned} &\omega_f(\tau) = \omega_r + (\omega_p - \omega_r)\left(\frac{\omega_s - \omega_r}{\omega_p - \omega_r}\right)^{\tau/t_{\max}} \qquad \zeta_f(\tau) = \alpha_f(\tau)/\omega_f(\tau) \\ &\alpha_f(\tau) = \omega_p\zeta_p + (\omega_r\zeta_r - \omega_p\zeta_p)\tau/t_{dur} \end{aligned} \tag{3}$$

with ω_p (primary wave frequency), ω_s (secondary wave frequency), ω_r (surface wave frequency), ζ_p (primary wave damping), and ζ_r (surface wave damping) ultimately corresponding to model parameters for the filter and t_{max} corresponding to the time at which maximum intensity of the ground motion is achieved and t_r to a sufficient time, chosen here to correspond to the time that 95% of the Arias intensity is reached. The time envelope $q(t, I_a, \alpha_2, \alpha_3)$ is given by (Rezaeian and Der Kiureghian 2010)

$$q(t, I_a, \alpha_2, \alpha_3) = \sqrt{I_a}\left[\sqrt{\frac{2}{\pi}\frac{(2\alpha_3)^{2\alpha_2-1}}{\Gamma(2\alpha_2-1)}}\right]t^{\alpha_2-1}\exp(-\alpha_3 t) \tag{4}$$

where $\Gamma(.)$ is the gamma function, I_a is the Arias intensity expressed in terms of g, and $\{\alpha_2, \alpha_3\}$ are additional parameters controlling the shape and total duration of the envelope that can be related to various physical parameters; here, the strong motion duration, $D_{5\text{-}95}$ (defined as the duration for the Arias intensity to increase from 5% to 95% of its final value), and the peak of the envelope function, λ_p, are used, through the following approach. For the modulating function in (4), the variance function $q^2(t, I_a, \alpha_2, \alpha_3)$ (related to Arias intensity) is proportional to a gamma probability function having parameter shape and scale parameters, $2\alpha_2$-1 and $1/(2\alpha_3)$ respectively (Rezaeian and Der Kiureghian 2008). If t_p represents the p-percentile variate of the gamma cumulative distribution function (this means that t_p is given in terms of the inverse of the gamma cumulative distribution function at probability value $p\%$) then it follows that t_p is uniquely given in terms of the parameters α_2 and α_3 and probability $p\%$. Then simply $D_{5\text{-}95}=t_{95}-t_5$. The value of λ_p is defined, based on the recommendations of (Boore 2003), as the ratio of time corresponding to the peak of the envelope in (4) to the time corresponding to 95% of its peak value. For some chosen $D_{5\text{-}95}$ and λ_p, α_2, and α_3 are selected through the solution of a nonlinear system of two equations satisfying this selection.

Ultimately, the ground motion model has as parameters $\boldsymbol{\theta}=\{D_{5\text{-}95}, \lambda_p, \omega_p, \omega_s, \omega_r, \zeta_p, I_a\}$ with the last one directly impacting (scaling) the output (thus input-output relationship is known) and the remaining six, denoted by $\mathbf{x}$ herein, having a complex nonlinear relationship to that output. Parameter ζ_r was found to have a small only impact on the structural response and as such has been taken in this study to take a constant value, 0.6.

The goal is then to derive a predictive relationship that will relate $\boldsymbol{\theta}$ to seismicity and soil characteristics. Though the approach can be extended to consider additional characteristics such as fault type or soil properties, the focus of this study will be on the moment magnitude, M, and the rupture distance, r_{rup}. In other words the predictive relationships are developed for specific fault type and local soil properties, and the goal is to then match the predictions for different seismicity characteristics (defined by M and r_{rup}). Based on the recommendations in (Travasarou and Bray 2003; Rathje, Faraj et al. 2004; Bommer, Stafford et al. 2009) the predictive relationships assumed here for the different model parameters are

$$\begin{aligned}
&\ln\left(I_a\right) = c_{1,1} + c_{1,2}M + c_{1,3}\ln\left(\sqrt{r_{rup}^{\ 2} + c_{1,5}^2}\right) + c_{1,4}\ln\left(M\right)\\
&\ln\left(D_{5-95}\right) = c_{2,1} + c_{2,2}M + c_{2,3}\ln\left(\sqrt{r_{rup}^{\ 2} + c_{2,4}^2}\right); \quad \ln\left(\lambda_p\right) = c_{3,1} + c_{3,2}M + c_{3,3}r_{rup}\\
&\ln\left(\omega_p / 2\pi\right) = c_{4,1} + c_{4,2}M + c_{4,3}r_{rup}; \quad \ln\left(\omega_s / 2\pi\right) = c_{5,1} + c_{5,2}M + c_{5,3}r_{rup};\\
&\ln\left(\omega_r / 2\pi\right) = c_{6,1} + c_{6,2}M + c_{6,3}r_{rup};\\
&\ln\left(\zeta_p\right) = c_{7,1} + c_{7,2}M + c_{7,3}r_{rup}
\end{aligned} \tag{5}$$

with the coefficients $c_{i,l}$ $i=1,...,6$, $l=1,...,5$ formulating the coefficient vector $\mathbf{c}$ that needs to be ultimately optimized to establish the compatibility to GMPEs. The general notation adopted to represent this transformation is $\boldsymbol{\theta} = G(M, r_{rup} \,|\, \mathbf{c})$.

KRIGING METAMODEL FORMULATION

For establishing the desired versatility in the optimization a kriging metamodel is adopted to approximate the average spectral acceleration, $SA_T(\boldsymbol{\theta})$, obtained through the stochastic ground motion model. This metamodel will ultimately provide a computational efficient approximation of the input-output relationship $\boldsymbol{\theta}$-$SA_T(\boldsymbol{\theta})$. Since the relationship to I_α is known, this pertains ultimately to the remaining parameters $\mathbf{x}$. A kriging metamodel is chosen here for this purpose, since it offers the best linear unbiased predictor. It is based only on matrix manipulations (providing great computational efficiency) and can facilitate an analytical evaluation of the gradient information, needed later in the optimization.

For forming the kriging metamodel initially, a database with n observations is obtained that provides information for the $\mathbf{x}$-$SA_T(\boldsymbol{\theta})$ pair. For this purpose n $(=10{,}000$ in the implementation considered later) samples for $\{\mathbf{x}^j\, j=1,..,n\}$, also known as *support points*, are created following a latin hybercube grid over the expected range of values possible for each x_i. Stochastic ground motions are then generated according to (1) and the peak acceleration of a linear SDOF oscillator with 5% damping (chosen to match the damping the GMPEs are calibrated for) with different values of structural period, T, is numerically evaluated. The influence of the white noise is addressed by considering 400 different samples for it (for each $\mathbf{x}^j$) and finally obtaining the average estimate to represent $SA_T(\boldsymbol{\theta})$. This ultimately provides the n_y dimensional output vector $\mathbf{y}(\mathbf{x}^j)$, corresponding to the peak spectral acceleration for the n_y different periods, T, considered, for each $\mathbf{x}^j$.

Using this dataset, the kriging model is then obtained. The fundamental building blocks of Kriging are the n_p dimensional basis vector, $\mathbf{f}(\mathbf{x})$, and the correlation function $R(\mathbf{x}^j,\mathbf{x}^k)$. Typical selections are made for both here, for the former a full quadratic basis and for the latter a generalized exponential correlation, leading to

$$\mathbf{f}(\mathbf{x})=[1\;\; x_1\;\cdots\; x_{n_x}\;\; x_1^2\;\; x_1x_2\;\cdots\; x_{n_x}^2\,];\quad n_p=(n_x+1)(n_x+2)/2$$

$$R(\mathbf{x}^j,\mathbf{x}^k)=\prod\nolimits_{i=1}^{n_x}\exp[-\varphi_i\,|\,\mathbf{x}_i^j-\mathbf{x}_i^k\,|^{\varphi_{n_x+1}}];\quad \boldsymbol{\varphi}=[\varphi_1\;\cdots\;\varphi_{n_x+1}] \tag{6}$$

Then for the set of n observations (training set) with input matrix $\mathbf{X}=[\mathbf{x}^1\,\ldots\,\mathbf{x}^n]^T$ and corresponding output $\mathbf{Y}=[\mathbf{y}^1\,\ldots\,\mathbf{y}^n]^T$, we define the basis matrix $\mathbf{F}=[\mathbf{f}(\mathbf{x}^1)\,\ldots\,\mathbf{f}(\mathbf{x}^n)]^T$ and the correlation matrix $\mathbf{R}$ with the jk-element defined as $R(\mathbf{x}^j,\mathbf{x}^k)$, j, $k=1,\ldots,n$. Also for every new input $\mathbf{x}$, we define the correlation vector $\mathbf{r}(\mathbf{x})=[R(\mathbf{x},\mathbf{x}^1)\,\ldots\,R(\mathbf{x},\mathbf{x}^n)]^T$ between the input and each of the elements of $\mathbf{X}$. Then the kriging approximation is given by (Lophaven 2002)

$$\overline{\mathbf{y}}(\mathbf{x})=\mathbf{f}(\mathbf{x})^T\boldsymbol{\alpha}^*+\mathbf{r}(\mathbf{x})^T\boldsymbol{\beta}^* \tag{7}$$

where the vectors $\boldsymbol{\alpha}^*$ and $\boldsymbol{\beta}^*$ are given by

$$\boldsymbol{\alpha}^*=(\mathbf{F}^T\mathbf{R}^{-1}\mathbf{F}\,)^{-1}\mathbf{F}^T\mathbf{R}^{-1}\mathbf{Y};\;\boldsymbol{\beta}^*=\mathbf{R}^{-1}(\mathbf{Y}-\mathbf{F}\boldsymbol{\alpha}^*) \tag{8}$$

Through the proper tuning of the parameters $\boldsymbol{\varphi}$ of the correlation function, kriging can efficiently approximate very complex functions. The optimal selection of $\boldsymbol{\varphi}$ is based on the Maximum Likelihood Estimation (MLE) principle, where the likelihood is defined as the probability of the n observations, and maximizing this likelihood with respect to $\boldsymbol{\varphi}$ ultimately corresponds to the optimization problem (Lophaven 2002)

$$\boldsymbol{\varphi}^*=\arg\min_{\boldsymbol{\varphi}}\left[\left|\mathbf{R}\right|^{\frac{1}{n}}\sum\nolimits_{j=1}^{n}\tilde{\sigma}_j^2\right] \tag{9}$$

where |.| stands for determinant of a matrix and $\tilde{\sigma}_j^2$ j=1,.., n correspond to the diagonal elements of matrix

$$\frac{(\mathbf{Y}-\mathbf{F}\boldsymbol{\alpha}^*)^T\mathbf{R}^{-1}(\mathbf{Y}-\mathbf{F}\boldsymbol{\alpha}^*)}{n} \tag{10}$$

The performance of the metamodel can be validated by calculating different error statistics using a leave-one-out cross-validation approach. This approach is established by removing sequentially each of the observations from the database, using the remaining support points to predict the output for that one and then evaluating the error between the predicted and real responses. The validation statistics are then obtained by averaging the errors established over all observations.

Ultimately, (7) provides a computational efficient approximation to the spectral acceleration for different natural periods (evaluation in the application considered here requires close to 0.1 sec). The computational intensive aspect of the entire formulation is the development of the database **Y** which requires time-history analysis for a large number of model parameters, to populate the entire region for which **x** is anticipated to take values in, and sufficient number of white noise samples, to address the resultant variability in the response. This needs to be performed, though, only once. As soon as the kriging metamodel is established based on this database, it can be then used to efficiently predict the responses for any other **x** desired.

OPTIMIZATION FOR PREDICTIVE RELATIONSHIPS

The objective is to ultimately select the coefficient vector **c** in the predictive relationships $\boldsymbol{\theta}=G(M,r_{rup}|\mathbf{c})$, utilizing the kriging metamodel for computational efficiency. The selection is based on matching the predictions for the spectral acceleration provided by the stochastic ground motion model to some target predictions, provided through GMPEs. As discussed earlier, the matching in this study is established over different seismicity characteristics, defined through the vector $\mathbf{z}=[M\ r_{rup}]^T$ and for different structural periods$T$. To formalize this idea, let **Z**=[$\mathbf{Z}=[\mathbf{z}^1\ldots\mathbf{z}^{n_s}]$ denote the matrix of the n_s seismicity cases considered, $\mathbf{T}=[T^1\ldots T^{n_t}]$ the vector of different structural periods chosen, and $\hat{S}_a(\mathbf{z},T)$ the target spectral acceleration for **z** and T provided through the GMPEs selected (note that instead of a specific GMPE this may correspond to the mean over a set of alternative GMPEs). Also, let $S_a(\mathbf{z},T)$ correspond to the average spectral acceleration provided through the stochastic ground motion model. This is ultimately evaluated by first transforming each sample for vector $\mathbf{z}^k$ to the model parameters $\boldsymbol{\theta}^k$ through the predictive Equations (5), then providing the kriging prediction (7) for $\mathbf{x}^k$ (corresponding to the 6 first components of $\boldsymbol{\theta}^k$) and ultimately setting

$$S_a(\mathbf{z},T)=\sqrt{I_a^k}\,\overline{\mathbf{y}}(\mathbf{x}^k) \tag{11}$$

where I_a^k corresponds to the last component of $\boldsymbol{\theta}^k$. Finally, the objective function for the optimization is defined by the weighted square error

$$f_{opt}=\frac{1}{n_s n_t}\sum\nolimits_{k=1}^{n_s}\sum\nolimits_{j=1}^{n_t}\gamma_{kj}^2\left(S_a(\mathbf{z}^k,T^j)-\hat{S}_a(\mathbf{z}^k,T^j)\right)^2 \tag{12}$$

where γ_{kj} corresponds to the weights penalizing the different error components. The vector $\mathbf{c}$ is then obtained by

$$\begin{aligned}&\mathbf{c}=\arg\min f_{opt}\\&\text{given }\ \mathbf{g}_{opt}(\mathbf{c})<0\end{aligned} \tag{13}$$

Where $\mathbf{g}_{opt}(\mathbf{c})$ corresponds to any additional constraints considered in the optimization. Such constraints correspond, for example, to the model parameters $\boldsymbol{\theta}$ constrained within pre-selected ranges for specific values of the vector $\mathbf{z}$, or to the coefficients $\mathbf{c}$ themselves satisfying box-bounded constraints.

The optimization (13) corresponds to a non-convex problem, and for finding the global optimum a two-stage optimization approach is adopted and implemented through the TOMLAB toolbox (Holmstrom, Goran et al. 2009). In the first stage of the optimization a direct search (gradient-free) is implemented to identify candidate local optima. Then in the second stage, a gradient-based optimization is performed to converge to the global optimum, using each of the previously identified candidate optima as a starting point. For improving the efficiency of the second stage, the gradient of the objective function is also analytically calculated. The components of this gradient are obtained as

$$\begin{aligned}\frac{\partial f_{opt}}{\partial c_{il}} &= 2\sum_{k=1}^{n_s}\sum_{j=1}^{n_t}\gamma_{kj}^2\left(S_a(\mathbf{z}^k,T^j)-\hat{S}_a(\mathbf{z}^k,T^j)\right)\left[\left.\frac{\partial S_a(\mathbf{z},T)}{\partial c_{il}}\right|_{\mathbf{z}=\mathbf{z}^k,T=T^j}\right] \\ &= 2\sum_{k=1}^{n_s}\sum_{j=1}^{n_t}\gamma_{kj}^2\left(S_a(\mathbf{z}^k,T^j)-\hat{S}_a(\mathbf{z}^k,T^j)\right)\left[\left.\frac{\partial S_a(\mathbf{z},T)}{\partial \theta_i}\right|_{\mathbf{z}=\mathbf{z}^k,T=T^j}\right]\left[\left.\frac{\partial \theta_i}{\partial c_{il}}\right|_{\mathbf{z}=\mathbf{z}^k}\right]\end{aligned} \tag{14}$$

where in the last equation the gradient in the second brackets is easily obtained from (5) whereas for the first one we have

$$\frac{\partial S_a(\mathbf{z},T)}{\partial \theta_i}=\frac{\partial\left(\sqrt{I_a}\,\overline{\mathbf{y}}(\mathbf{x})\right)}{\partial \theta_i}=\begin{cases}\sqrt{I_a}\,\dfrac{\partial \overline{\mathbf{y}}(\mathbf{x})}{\partial x_i} & \text{if } i=1,\ldots,5\\ -\overline{\mathbf{y}}(\mathbf{x})/2\sqrt{I_a} & \text{if } i=6\end{cases} \tag{15}$$

with the derivative for the kriging model $\partial\overline{\mathbf{y}}(\mathbf{x})/\partial x_i$ readily obtained through (7) since and the value of x_i only influencing vectors $\mathbf{f}(\mathbf{x})$ and $\mathbf{r}(\mathbf{x})$, not vectors $\boldsymbol{\alpha}^*$ and $\boldsymbol{\beta}^*$ (Lophaven 2002).

ILLUSTRATIVE IMPLEMENTATION

For the illustrative implementation n=5,000 support points are used to develop the kriging metamodel. The support points are selected utilizing latin hypercube sampling in the following ranges, [0.5 *s* 55*s*] for $D_{5\text{-}95}$, [0.01 0.6] for λ_p, [10*Hz* 50 *Hz*] for $\omega_p/2\pi$, [2*Hz* 20 *Hz*] for $\omega_s/2\pi$, [0.1*Hz* 5 *Hz*] for $\omega_r/2\pi$, and [0.01 0.3] for ζ_p. The response for each support point is averaged over 400 white-noise samples to obtain the average statistics. The outputs for which the metamodel is developed include the peak spectral acceleration for periods T =[0 0.01 0.02 0.03 0.04 0.05 0.075 0.1 0.15 0.2 0.25 0.3 0.4 0.5 0.75 1.0 1.5 2.0 3.0 4.0 5.0 7.5 10.0] *s*. The average (over all the outputs) absolute mean error established for the metamodel is 2% which corresponds to very good accuracy, whereas each new prediction for the metamodel (for a new $\mathbf{x}$) takes an average of $0.1\,s$ for the entire output vector. For generating the total of 4,000,000 time histories and performing the required 46,000,000 simulations to develop the database for the metamodel, close to 10,000 CPU hours were required. Though this computational burden is significant, it corresponds to an initial only overhead of the approach, as illustrated in Figure 1 earlier. Once the metamodel is developed, it can be then used for any required predictions since the established accuracy is high. The large number of support points was selected primarily with this aspect in mind, so that a high-accuracy threshold is guaranteed for an extensive range of values for $\mathbf{x}$. The metamodel can be then used to establish a match to GMPEs with different characteristics and, to demonstrate this versatility, three different cases are considered. For all cases the match is provided for local site conditions corresponding to shear wave velocity V_s=600 *m*/*s* and a strike-slip fault. For the first case, the average of four different GMPEs is considered, the ones developed for crustal earthquakes in the Western U.S. (Abrahamson and Silva 2008; Boore and Atkinson 2008; Campbell and Bozorgnia 2008; Chiou and Youngs 2008) with the seismicity characteristics for $\mathbf{z}$ defined as the combination of [5 6 7 8] for M and [10 30 50] for r_{rup}, and T

chosen as [0.3 0.4 0.5 0.75] s. Thus n_s=12 and n_t=4. Since many of the chosen GMPEs require additional seismicity inputs, beyond M and r_{rup}, the nominal relationships suggested in (Kaklamanos, Baise et al. 2011) are used to derive these inputs, starting from the M and r_{rup} values. For the second and third case, the target is only the (Abrahamson and Silva 2008) GMPE. For the second case the assumptions are the same as for the first one, whereas the third assumes a greater range of periods for which the match is established, with T corresponding to [0.1 0.2 0.3 0.4 0.5 0.75 1 1.5 2 3] s and thus n_t=10.

The optimization is then performed for all three cases, with weighting coefficient γ_{kj} chosen equal to $1/\hat{S}_a(\mathbf{z}^k, T^j)$, thus establishing a normalization of the output. The optimal values of the objective function are, respectively, 0.004, 0.0112, and 0.1131. As expected Case 1 and 2 yield lower levels of accuracy, whereas for Case 3 (targeting a greater range of periods) this accuracy deteriorates. The time needed to perform the optimization is 500 s, whereas if the second stage was only performed the respective requirement is 10 s, but in this case a local minimum is only guaranteed to be obtained. The established predictive relationships for the three cases are shown in Figure 2, whereas the results for the match are presetned in Figure 3 and Figure 4. In particular, Figure 3 reports the PSA for the different M, r_{rup} configurations and for different values of T (curves in each figure) for the three cases (columns in the figure). The estimates for the GMPEs as well as of the optimized stochastic ground motion model are presented (rows in the figure). To validate the accuracy of the kriging approximation, for the latter the estimates coming from the metamodel, as well as the estimates from direct implementation of the ground motion model (again averaging over 400 white noise sequences) are both reported. Figure 4 shows spectral plots (for all T considered) in a similar fashion, for specific values of M and r_{rup}.

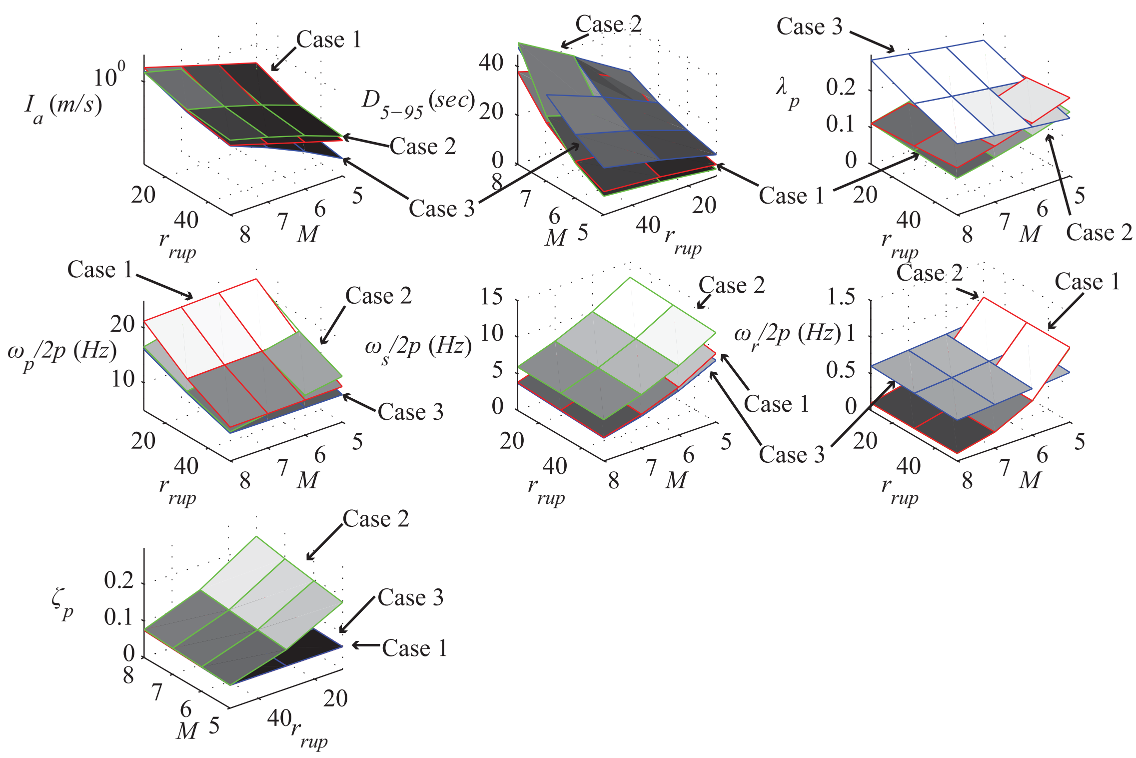

Figure 2. Predictive relationships for all model parameters

The predictive relationships (Figure 2) are in good agreement with the trends provided by direct observations or recorded ground motions (Travasarou and Bray 2003; Rathje, Faraj et al. 2004; Bommer, Stafford et al. 2009). This is an important feature, showing that the matching to GMPEs does not yield non-physical model characteristics. When looking at the accuracy of the predictions by the stochastic ground motion model (Figure 3-Figure 4) the good match to the targeted predictions is verified. Case 3 encounters, as expected greater challenges, whereas the predictions of the stochastic ground motion model coming from direct simulation and through the metamodel approximation exhibit an overall close agreement, something that validates the accuracy of the surrogate model and ultimately of the entire framework advocated here (Figure 1).

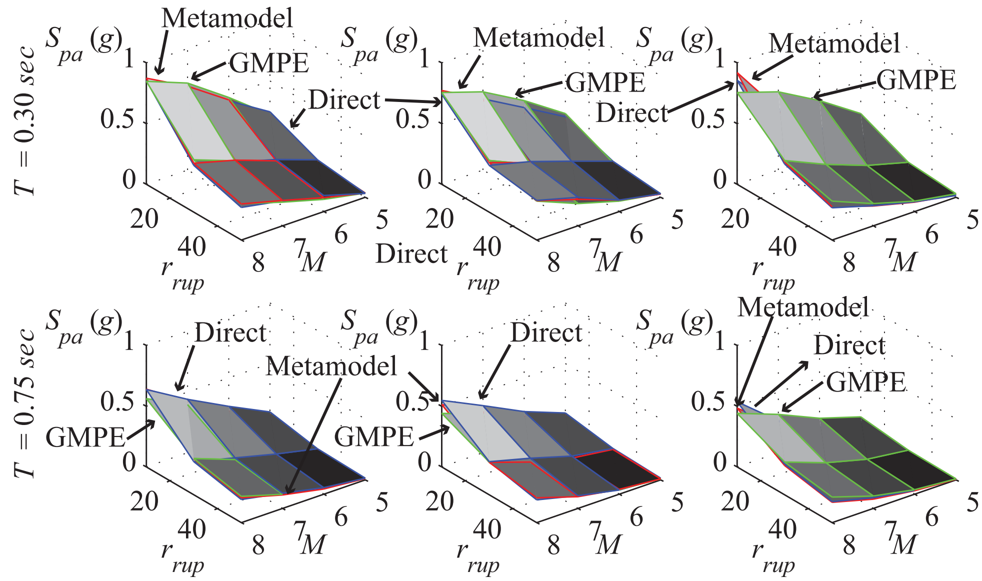

Figure 3. Comparison of PSA predictions by the stochastic ground motion model to the targeted ones (provided by the GMPEs) for different M and r_{rup} for two different periods. For the stochastic ground motion model, "direct" corresponds to evaluation by simulation and "metamodel" to estimation through the surrogate model.

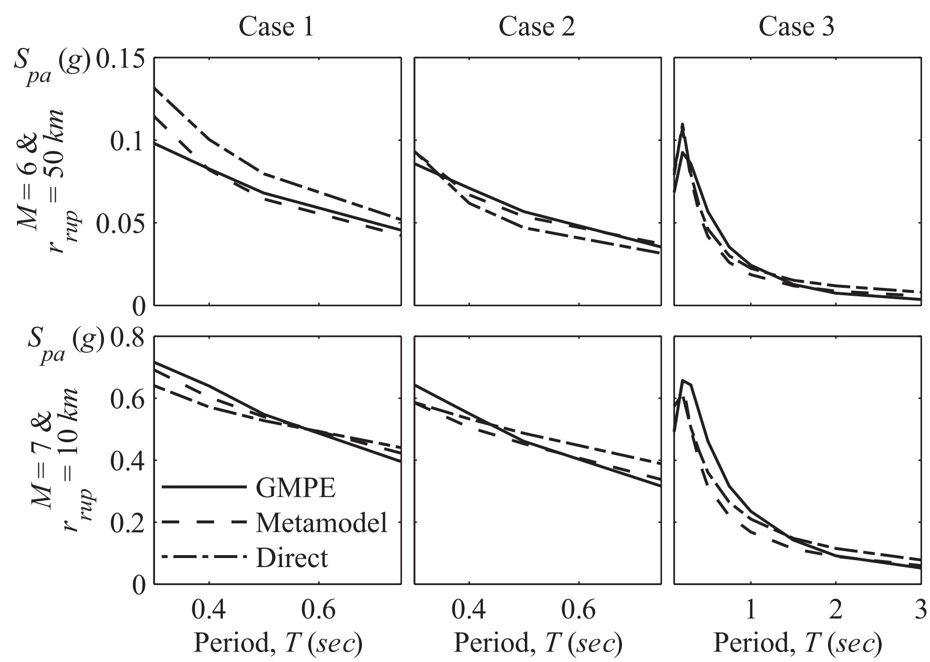

Figure 4. Comparison of PSA predictions by the stochastic ground motion model to the targeted ones (provided by the GMPEs) for different periods for two M, r_{rup} combinations. Legend terminology is same as in Figure 3.

The optimized ground motion models can be now used to develop acceleration time-histories compatible with the chosen GMPEs. Figure 5 shows such sample time histories for three different events $\{M=6,\ r_{rup}=10\,km\}$, $\{M=7,\ r_{rup}=50\,km\}$ and $\{M=8,\ r_{rup}=30\,km\}$ for the three different cases considered.

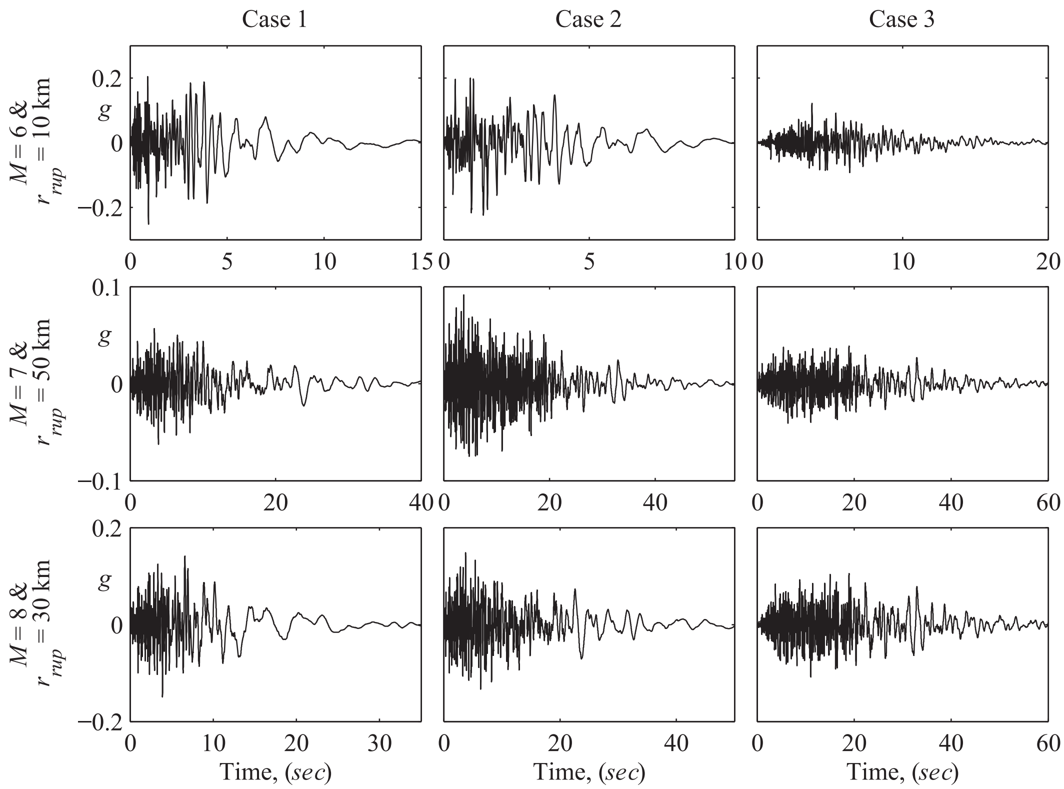

Figure 5. Sample time histories provided by the optimized stochastic ground motion model

CONCLUSIONS

With the growing interest in the last decade on PBEE, the need for reliable models to characterize acceleration time histories of seismic excitations has intensified. Motivated by this realization, the tuning of stochastic ground motion models to provide predictions compatible with GMPEs was discussed in this paper. This was established by optimizing the coefficients of the predictive relationships in these models that relate model parameters to seismicity characteristics. A model that addresses both temporal and spectral non-stationarities was selected as stochastic ground motion model in the illustrative example. Foundation of the approach is the development of a metamodel (surrogate model) that provides an efficient and accurate approximation of the average responses from this model. Though the initial computational overhead for development of the database, required for this metamodel, is substantial, the optimized surrogate model (chosen here to correspond to a kriging metamodel) can be utilized to facilitates an efficient optimization to match any desired GMPE for any chosen seismicity characteristics and structural properties (structural period). The computational efficiency of the approach can be further exploited for the development of standalone-apps that will facilitate the generation of ground motions compatible with a specific GMPE for a specific structure and region (defining local site conditions, fault-type and periods of interest) allowing the end-user to ultimately make these choices, which is the long term goal of this research.

In the illustrative example presented the following observations can be made: The proposed metamodel approach facilitates an efficient optimization of the coefficients of the predictive relationships to match any desired GMPE or combination, as shown between Case 1 and Case 2. Furthermore, the efficiency of this approach can be exploited to allow the optimization to specific or range structures (periods) and sites of interest, thus allowing for specific site and structure hazard compatible ground motions, as shown in the comparison between cases 2 and 3. Finally, the accuracy of the metamodel, evaluated through the direct simulation of the stochastic ground motion model and predictions from the metamodel, is shown to be well within a desired range when considering different seismicity levels and structures of interest.

REFERENCES

Abrahamson, N. and W. Silva (2008). "Summary of the Abrahamson & Silva NGA ground-motion relations." Earthquake Spectra 24(1): 67-97.

Au, S. K. and J. L. Beck (2003). "Subset simulation and its applications to seismic risk based on dynamic analysis." Journal of Engineering Mechanics, ASCE 129(8): 901-917.

Baker, J. W. and C. A. Cornell (2005). "A vector-valued ground motion intensity measure consisting of spectral acceleration and epsilon." Earthquake Engineering and Structural Dynamics 34(10): 1193-1217.

Beck, J. L. and C. Papadimitriou (1993). "Moving resonance in nonlinear response to fully nonstationary stochastic ground motion." Probabilistic Engineering Mechanics 8(3-4): 157-167.

Bommer, J. J., P. J. Stafford, et al. (2009). "Empirical Equations for the Prediction of the Significant, Bracketed, and Uniform Duration of Earthquake Ground Motion." Bulletin of the Seismological Society of America 99(6): 3217-3233.

Boore, D. M. (2003). "Simulation of ground motion using the stochastic method." Pure and Applied Geophysics 160: 635-676.

Boore, D. M. and G. M. Atkinson (2008). "Ground-motion prediction equations for the average horizontal component of PGA, PGV, and 5%-damped PSA at spectral periods between 0.01 s and 10.0 s." Earthquake Spectra 24(1): 99-138.

Campbell, K. W. and Y. Bozorgnia (2008). "NGA ground motion model for the geometric mean horizontal component of PGA, PGV, PGD and 5% Damped linear elastic response spectra for periods ranging from 0.01 to 10 s." Earthquake Spectra 24(1): 139-171.

Chiou, B. S. J. and R. R. Youngs (2008). "An NGA model for the average horizontal component of peak ground motion and response spectra." Earthquake Spectra 24(1): 173-215.

Dabaghi, M., S. Rezaeian, et al. (2011). Stochastic simulation of near-fault ground motions for specified earthquake and site characteristics. 11th International Conference on Applications of Statistics and Probability in Civil Engineering. Zurich, Switzerland.

Gavin, H. P. and B. W. Dickinson (2011). "Generation of uniform-hazard earthquake ground motions " Journal of Structural Engineering, ASCE 137(3): 423-432.

Goulet, C. A., C. B. Haselton, et al. (2007). "Evaluation of the seismic performance of code-conforming reinforced-concrete frame building-From seismic hazard to collapse safety and economic losses." Earthquake Engineering and Structural Dynamics 36(13): 1973-1997.

Grigoriu, M. (2011). "To scale or not to scale seismic ground-acceleration records." Journal of Engineering Mechanics, ASCE 137(4): 284-293.

Holmstrom, K., A. O. Goran, et al. (2009). User's guide for TOMLAB 7. San Diego, CA, Tomlab Optimization Inc. www.tomopt.com/tomlab/.

Jalayer, F. and J. L. Beck (2008). "Effects of two alternative representations of ground-motion uncertainty in probabilistic seismic demand assessment of structures." Earthquake Engineering and Structural Dynamics 37(1): 61-79.

Kaklamanos, J., L. G. Baise, et al. (2011). "Estimating Unkown Input Parameters when Implementing the NGA Ground-Motion Prediction Equations in Engineering Practice." Earthquake Spectra 27(4): 1219-1235.

Lophaven, S. N., Nielsen, H.B., and Sondergaard, J. (2002). DACE-A MATLAB Kriging Toolbox, Technical University of Denmark.

Papadimitriou, K. (1990). Stochastic characterization of strong ground motion and application to structural response. Pasadena, CA, Report No. EERL 90-03, California Institute of Technology.

Rathje, E. M., F. Faraj, et al. (2004). "Empirical Relationships for Frequency Content Parameters of Earthquake Ground Motions." Earthquake Spectra 20(1): 119-144.

Rezaeian, S. and A. Der Kiureghian (2008). "A stochastic ground motion model with separable temporal and spectral nonstationatiries." Earthquake Engineering & Structural Dynamics 37: 1565-1584.

Rezaeian, S. and A. Der Kiureghian (2010). "Simulation of synthetic ground motions for specified earthquake and site characteristics." Earthquake Engineering & Structural Dynamics 39(10): 1155-1180.

Scherbaum, F., F. Cotton, et al. (2006). "The estimation of minimum-misfit stochastic models from empirical ground-motion prediction equations." Bulletin of the Seismological Society of America 96(2): 427-445.

Taflanidis, A. A. (2011). Soft computing applications in simulation-based natural hazard risk assessment Soft Computing Methods for Civil and Structural Engineering. Y. Tsompanakis and B. H. V. Topping, Saxe-Coburg Publications.

Taflanidis, A. A. and G. Jia (2011). "A simulation-based framework for risk assessment and probabilistic sensitivity analysis of base-isolated structures." Earthquake Engineering & Structural Dynamics 40: 1629–1651.

Taflanidis, A. A., C. Vetter, et al. (2013). Stochastic ground motion modeling: opportunities and challenges for seismic hazard description in probabilistic risk assessment. 11th International Conference on Structural Safety & Reliability. New York, NY.

Travasarou, T. and J. D. Bray (2003). "Empirical attenuation relationship for Arias intensity." Earthquake Engineering & Structural Dynamics 32(7): 1133–1155.

Vetter, C. and A. Taflanidis (2014). "Comparison of alternative stochastic ground motion models for seismic risk characterization." Soil Dynamics and Earthquake Engineering 58: 48-65.

Yamamoto, Y. and J. W. Baker (2013). "Stochastic Model for Earthquake Ground Motion Using Wavelet Packets." Bulletin of the Seismological Society of America 103(6): 3044-3056.